

# Highly photostable solid-state dye lasers based on silicon-modified organic matrices

A. Costela<sup>a)</sup> and I. García-Moreno

*Instituto de Química Física "Rocasolano," CSIC, Serrano 119, 28006 Madrid, Spain*

D. del Agua, O. García, and R. Sastre

*Instituto de Ciencia y Tecnología de Polímeros, CSIC, Juan de la Cierva 3, 28006 Madrid, Spain*

(Received 16 May 2006; accepted 5 July 2006; published online 13 April 2007)

We report on the synthesis, characterization, and physical properties of modified polymeric matrices incorporating silicon atoms in their structure and doped with laser dyes. When the silicon-modified organic matrices incorporated pyrromethene 567 (PM567) and pyrromethene 597 (PM597) dyes as actual solid solutions, highly photostable laser operation with reasonable, nonoptimized efficiencies was obtained under transversal pumping at 532 nm. At a pump repetition rate of 10 Hz, the intensity of the laser emission remained at the level or above the initial lasing intensity after 100 000 pump pulses in the same position of the sample, corresponding to an estimated accumulated pump energy absorbed by the system of 518 and 1295 GJ/mol for PM567 and PM597, respectively. When the pump repetition rate was increased to 30 Hz, the laser emission of dye PM567 decreased steadily and the output energy fell to one-half its initial value after an accumulated pump energy of 989 GJ/mol. Dye PM597 demonstrated a remarkable photostability, and under 30 Hz pumping the laser emission from some samples remained stable after 700 000 pump pulses in the same position of the sample, corresponding to an accumulated pump energy of 17 300 GJ/mol. Narrow linewidth operation with tuning ranges of up to 31 nm was obtained with both pyrromethene dyes when some of the samples were incorporated into a grazing-incidence grating oscillator. © 2007 American Institute of Physics. [DOI: 10.1063/1.2359117]

## I. INTRODUCTION

The use of solid matrices incorporating laser dyes to build practical, tunable, solid-state dye lasers is an attractive alternative to liquid dye lasers.<sup>1</sup> Solid-state dye lasers, while retaining the versatility of liquid dye lasers, avoid the need to handle large volumes of messy and sometimes toxic liquids, present a low-cost gain medium, and are easy to operate and maintain. They allow for the design of compact and self-contained laser systems, which will facilitate their utilization in industrial or medical environments.

Organic polymers have been attractive materials used as solid hosts for lasing dyes since they exhibit good solubility and chemical compatibility with organic dyes, as well as excellent optical homogeneity, which is important to avoid interference in the gain medium due to microscopic variations in the refractive index.<sup>2,3</sup> Polymers are adaptable to inexpensive fabrication techniques, and the easiness with which relevant characteristics of these materials such as free volume, chemical composition, molecular weight, microstructure, and viscoelasticity can be modified in a controlled way facilitates the optimization of their properties to be used in specific applications.<sup>1,4</sup>

Counterbalancing the aforementioned advantages, photodegradation of polymeric dye laser materials, due to the low power-damage threshold of the matrix and the photo- and thermally induced changes of the emitting dye during the excitation process, can be an important limitation in the use

of organic polymeric matrices as hosts for lasing dyes. In addition, thermal lensing effects, which depend on the linear thermal coefficient of refractive index  $\partial n/\partial T$ , can be quite severe in some polymers due to the relatively high values of  $\partial n/\partial T$  in these media, of the order of  $-10^{-4} \text{ K}^{-1}$ .<sup>5,6</sup> Thus, concave or negative, thermal lenses with focal lengths in the few centimeter range have been observed in polymeric solid-state dye lasers in the pulsed regime at pump power densities of  $\sim 0.5 \text{ J/cm}^2$ .<sup>7</sup>

One approach to improve the thermal properties of the laser material without losing the benefits provided by polymers has been the use of organic-inorganic hybrid materials.<sup>3,8-16</sup> However, these materials present their own problems such as complex and lengthy synthesis process, fragility which makes mechanization of the final material difficult, and most important, optical inhomogeneity caused by refractive index mismatch between organic and inorganic parts.

Recently, Duarte and James<sup>17,18</sup> demonstrated a class of dye-doped, organic-inorganic, solid-state gain media that exhibit lower  $|\partial n/\partial T|$  values and improved optical homogeneity than previous composite gain media. The gain media consisted of silica nanoparticles uniformly dispersed in poly(methyl methacrylate) (PMMA), and high laser conversion efficiencies with low-beam divergence were obtained.

In this paper we report on an approach different from that of Duarte and James to improve the optical and mechanical properties of composite gain media while maintaining the advantages of combining polymer and inorganic materials. The basic idea is to use organic compounds with

<sup>a)</sup>Electronic mail: acostela@iqfr.csic.es

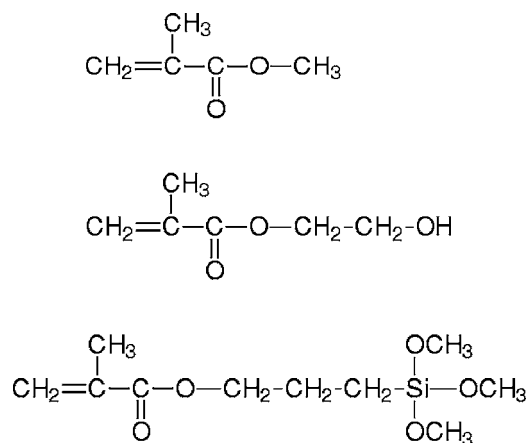


FIG. 1. Molecular structures of monomers MMA, HEMA, and TMSPMA.

silicon atoms incorporated into their structure. The matrix would remain organic, which means plasticity and a relatively more simple synthesis procedure, but with improved thermal properties due to the presence of the silicon atoms. We describe in some detail the preparation of the silicon-modified organic matrices incorporating lasing dyes; characterize their structural and physical properties by using methods such as Fourier transform infrared spectroscopy (FTIR), nuclear magnetic resonance (NMR), size exclusion chromatography (SEC), differential scanning calorimetry (DSC), thermogravimetry analysis (TGA), and refractometry; and evaluate their laser performance under static transversal pumping at 532 nm at 10 and 30 Hz repetition rates. Pyromethene 567 (PM567) and Pyromethene 597 (PM597) were chosen as reference dyes because there were previous studies on the lasing performance of these dyes in polymer, inorganic, and hybrid hosts, which would facilitate the evaluation of our results by comparison with those reported in the literature. Some preliminary results of the laser behavior here studied have been concisely reported in a previous letter.<sup>19</sup>

## II. EXPERIMENT

### A. Materials

PM567, PM597 (both laser grade from Exciton), and Rh6G (chloride salt, laser grade, Lambda Physik) dyes were used as received. Matrices based on copolymers and terpolymers of methacrylic monomers with monomers containing silicon atoms in their backbone were prepared. Methacrylic monomers used were MMA and 2-hydroxyethyl methacrylate (HEMA), both purchased from Aldrich and purified before use. Copolymers and terpolymers of these monomers with 3-(trimethoxysilyl)propyl methacrylate (TMSPMA) (Aldrich, 99% purity) were prepared. Figure 1 shows the molecular structures of these monomers. The dyes were incorporated into copolymers COP(MMA-TMSPMA  $x:y$ ) and COP(HEMA-TMSPMA  $x:y$ ), and into terpolymers TERP(MMA-HEMA-TMSPMA  $x:y:z$ ), with different monomer volumetric proportions  $x,y,z$ . In the copolymers, volumetric  $x:y$  proportions ranged from 9:1 to 3:7. In the terpolymers, volumetric  $x:y:z$  proportions used were 7:3:10, 5:5:10, and 3:7:10.

The synthesis route followed to prepare the materials studied in this work was the block radical polymerization of the above monomers. The organic polymerization was carried out by radical bulk polymerization using 2,2'-azobis(isobutyronitrile) (AIBN) in an appropriate concentration (0.5 wt %) with regard to the total amount of organic monomers in the polymerization mixture. AIBN is the thermal polymerization initiator of choice, since it leaves ultraviolet-transparent end groups on the copolymer. It was purchased from Aldrich and was recrystallized in ethanol before use.

The adequate amount of the dye was added to freshly distilled TMSPMA, and the resulting mixture was placed in an ultrasonic bath until complete dissolution of the dye. We prepare a number of mixtures with different volume/volume proportions of monomers. The resulting solution was filtered into appropriate cylindrical polypropylene molds using a 2  $\mu\text{m}$  pore size filter [Whatman Lab, polytetrafluoroethylene (PTFE) disposable filters]. Polymerization was performed in a thermal bath at 40° over a period of 2 days and then at 45 °C for about 1 day. Afterwards the temperature was raised to 50 °C and increased slowly up to 80 °C over a period of 1 day, in order to decompose residual AIBN. Finally, the temperature was reduced in steps of 5 °C/day until room temperature was reached, and only then was the sample unmolded. This procedure was essential in order to reduce the buildup of stress in the polymer sample due to thermal shock.

To obtain the monomer reactivity ratio, and only in this case, the copolymerization reactions were carried out in solutions of toluene in glass vessels provided with rubber septa. Comonomer mixtures MMA-TMSPMA in v/v proportions ranging from 9:1 to 1:9 were prepared. The copolymerizations were carried out using AIBN as initiator at a constant temperatures of  $65 \pm 0.1$  °C. Copolymerization system was homogeneous in all cases investigated. After 30 min of reaction each reactor vessel was removed from the thermostatted water bath. Conversions were kept under 10% in all cases. The solutions were poured in an excess of heptane under vigorous stirring. Once the copolymer was precipitated the mixture was filtered and the obtained solid was washed with heptane. After that the copolymer was dried under reduced pressure until a constant weight was attained. A similar preparation procedure was followed with the other copolymers.

### B. Characterization

Infrared spectra of the samples as powder-pressed KBr pellets were recorded on a Fourier transform infrared spectrophotometer (spectrum RX I FTIR system, Perkin Elmer) in the spectral range of 4000 to 400  $\text{cm}^{-1}$ .

Molecular weights and molecular weight distributions were measured by SEC using a chromatography system (Waters Division Millipore) equipped with a Waters Model 410 refractive index detector. Tetrahydrofuran (THF) was used as an eluent at a flow rate of 1  $\text{cm}^3/\text{min}$ . The operation temperature was 35 °C. Styragel-packed columns (HR1, HR3, HR4E, and HR5E) were used. Calibration of the instrument

was performed with standard samples of PMMA (Polymer Laboratories) in the range between  $3.53 \times 10^6$  and  $5 \times 10^2$  g/mol.

The glass transition temperature ( $T_g$ ) of the silicon-modified matrices was determined by using a differential scanning calorimeter (DSC-6, Perkin Elmer). DSC scans of the materials as very fine powder were conducted under nitrogen atmosphere at a heating rate of  $20^\circ\text{C}/\text{min}$ , from  $-20$  to  $150^\circ\text{C}$ , after maintaining the material in vacuum for 5 h at  $30^\circ\text{C}$ . Thermogravimetric analysis of the materials, also as very fine powder, were performed on a thermogravimetry analyzer (TGA 7, Perkin Elmer) under nitrogen atmosphere at a heating rate of  $5^\circ\text{C}/\text{min}$  (copolymers of MMA with TMSPMA) or  $10^\circ\text{C}/\text{min}$  (materials containing HEMA), from  $20$  to  $800^\circ\text{C}$ .

Refractive indices of the prepared samples were measured at room temperature using an Abbe refractometer (Zeiss) employing 1-bromonaphthalene as sample-support interphase and a sodium lamp as monochromatic light at 589 nm.

$^1\text{H}$ -NMR (nuclear magnetic resonance) spectra were recorded at 300 MHz on a Bruker 300 spectrometer (Bruker Analytic GmbH) with deuterated chloroform. The relative signal intensities of the spectra were measured from the integrated peak area.

$^{29}\text{Si}$ -NMR experiments were performed in a Bruker Avance<sup>TM</sup> 400 spectrometer equipped with a Bruker Ultrashield<sup>TM</sup> 9.4 T ( $^{29}\text{Si}$  resonance frequency of 79.49 MHz), 8.9 cm vertical-bore superconducting magnet. The  $^{29}\text{Si}$  cross polarization magic angle spinning (CP-MAS) NMR spectra were obtained with 4 ms CP contact time, 5 s recycle delay, 6000 averages, and 75 Hz line broadening. The spectra were deconvoluted by using Gaussian fits, in terms of  $T^i$ , where  $i=1,2,3$ , corresponding to the number of siloxane bridges bonded to the silicon atom of interest.

In both cases, CP-MAS NMR spectra were acquired at ambient temperature by using a standard Bruker broadband MAS probe. Representative samples were grounded and packed in 4 mm zirconia rotors, sealed with Kel-F<sup>TM</sup> caps and spun at 5 kHz. The  $90^\circ$  pulse width was 3.5–4.5  $\mu\text{s}$  and, in all cases, high-power proton decoupling was used. All free induction decays were subjected to standard Fourier transformation and phasing. The chemical shifts were externally referenced to tetramethylsilane. The NMR spectra were evaluated with the software package XWIN-NMR<sup>TM</sup> provided by Bruker.

### C. Laser evaluation

The obtained cylindrical solid laser samples formed rods of 10 mm diameter and 10 mm length. A cut was made parallel to the axis of the cylinder in order to obtain a lateral flat surface of  $\sim 4 \times 10$  mm<sup>2</sup>. All flat surfaces were prepared for lasing experiments by conventional grinding and polishing. The samples were transversely pumped at 532 nm with 5.5 mJ and 6 ns full width at half maximum (FWHM) pulses from a frequency-doubled  $Q$ -switched Nd:yttrium aluminum garnet (YAG) laser (Spectron SL248G) at a repetition rate of 10 Hz. Some samples were pumped at 30 Hz with 3.5 mJ,

10 ns FWHM pulses from a diode pumped, frequency doubled,  $Q$ -switched Nd:YAG laser (Monocrom HALAZEN 532-12) The exciting pulses were line focused onto the lateral flat surface of the solid samples, and typical pump fluences on the active medium were  $180$  mJ/cm<sup>2</sup>. The oscillation cavity consisted of a 90% reflectivity aluminium mirror and the end face of the sample as the output coupler, with a cavity length of 2 cm. Details of the experimental setup can be found elsewhere.<sup>20</sup>

Narrow linewidth laser emission and tuning ranges of some of the dye-doped matrices were obtained by placing the samples in a homemade Shoshan-type oscillator<sup>21</sup> consisting of full reflecting aluminium back and tuning mirrors and a 2400 lines/mm holographic grating in grazing incidence, with outcoupling via the grating zero order. Laser linewidth was measured with a Fabry-Perot etalon (IC Optical Systems) with free spectral range of 15.9 GHz.

The dye and pump laser pulses were characterized with the following instruments: GenTec ED-100A and ED-200 pyroelectric energy meters, ITL TF1850 fast rise time photodiode, Tektronix 7934 storage oscilloscope, TDS3032 digital phosphor oscilloscope, and SpectraPro-300i spectrograph/monochromator (Acton Research Corporation) with charge-coupled device (CCD) (SpectruMM:GS128B) and Hamamatsu R928 photomultiplier. Dye and pump laser signals were sampled with boxcars (Stanford Research, model 250), and all the integrated signals were digitized and processed using a PC via a Computerboard DASH-8 interface.<sup>22</sup>

## III. RESULTS AND DISCUSSION

Three different kinds of matrices were used in the laser studies: copolymers of MMA or HEMA with TMSPMA and terpolymers of MMA, HEMA, and TMSPMA. In the copolymers, the proportion of TMSPMA present in the sample was varied and the effect of this variation on the dye laser operation was assessed. In the terpolymers, the amount of the silicon-containing monomer TMSPMA was kept constant and the relative proportion of the organic monomers MMA and HEMA was varied.

### A. Structural and physical properties of the silicon-modified organic matrices

Absorption and transmittance spectra of MMA and TMSPMA were identical over the visible range. In the infrared spectra of the prepared materials absorption characteristic bands can be seen in the ranges of 1000–1110 and 1170–1220 cm<sup>-1</sup>, which correspond to vibrations of Si–O–Si bonds and of Si–O–CH<sub>3</sub> bonds, and at 2840 and 3690 cm<sup>-1</sup>, which correspond to vibrations of Si–O–CH<sub>3</sub> bonds and of Si–OH bonds, respectively.<sup>23</sup> The intensity of the Si–OH and Si–O–Si bonds increases with the content of the silicon-containing monomer in the matrix and indicate a certain degree of hydrolysis and condensation between the alkoxide groups of TMSPMA.

The  $^{29}\text{Si}$  NMR spectra of copolymers COP(MMA-TMSPMA) (Fig. 2) confirm the above assignments. Two signals, at  $-42$  and  $-49$  ppm, were observed for each matrix assayed. The assignment of these peaks is based on previous

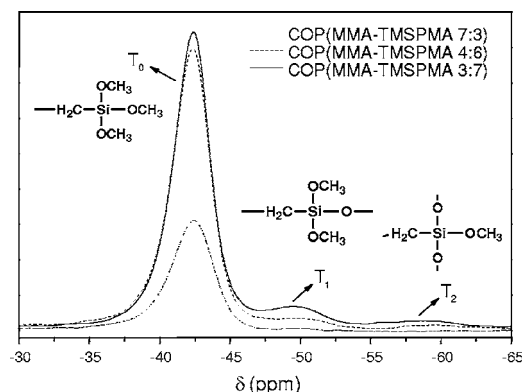


FIG. 2.  $^{29}\text{Si}$ -NMR spectra of copolymers of MMA and TMSPMA with different  $x:y$  monomer proportions.

studies on silica gel.<sup>24</sup> The peak at  $-42$  ppm corresponds to the  $T_0$  species and is attributed to the silicon atom bonded to three trimethoxy groups represented by  $-\text{CH}_2\text{Si}(\text{OCH}_3)_3$ . The peak  $T_1$  at  $-49$  ppm is related to the presence of a siloxane group bonded to the inorganic structure of type  $-\text{CH}_2\text{Si}(\text{OCH}_3)_2\text{O}-$ . Finally, the  $T_2$  peak at  $-59$  ppm, which barely appears in material COP(MMA-TMSPMA 3:7), is associated with silicon bonded to two siloxane groups, such as  $-\text{CH}_2\text{Si}(\text{OCH}_3)_2\text{O}_2-$ .

On the basis of the quantitative relationships of the signals, which are comparable under the same experimental conditions, it can be concluded from Fig. 2 that this type of polymers exhibits a slow but progressive increment of the inorganic degree of crosslinking as the proportion of TMSPMA in the material increases: the growth of the proportion of the  $T_1$  groups from 1.6% to 7.9% when the proportion of TMSPMA increases from 30 to 70 vol % confirms the presence of Si-O-Si and, thus, the occurrence of a certain cross-linking. No further peaks appeared in the CP-MAS  $^{29}\text{Si}$ -NMR spectra due to the presence of silicon bonded to an inorganic group in the different chemical environments studied.

The copolymer distribution in the silicon-modified organic matrices was random, with one silicon atom per TMSPMA monomer repetition unit, which appears as a side substituent (Fig. 1). The densities of the different compounds, which were determined using a conventional gravimetric method at room temperature, varied between 1.17 and 1.20 g/cm<sup>3</sup>, depending on the particular matrix composition.

Free radical copolymerizations of MMA with TMSPMA were carried out in 1.69M toluene solutions and  $1.5 \times 10^{-2}M$  of AIBN as initiator at 65 °C for 30 min. Conversions lower than 10% were obtained to satisfy the differential copolymerization equation. The average molar fraction composition of copolymer was quantitatively determined from the corresponding  $^1\text{H}$ -NMR spectra of copolymer samples prepared with different monomer feeds, taking the signal between 0.5 and 0.7 ppm, corresponding to the protons in the Si-CH<sub>2</sub>-group in the TMSPMA, and the signals between 3.40 and 3.70 ppm, corresponding to the protons in the O-CH<sub>3</sub> ester group in the MMA and to the protons in the Si-O-CH<sub>3</sub> group in the TMSPMA, respectively (Fig. 3). The conversion, the molar fraction composition of the mono-

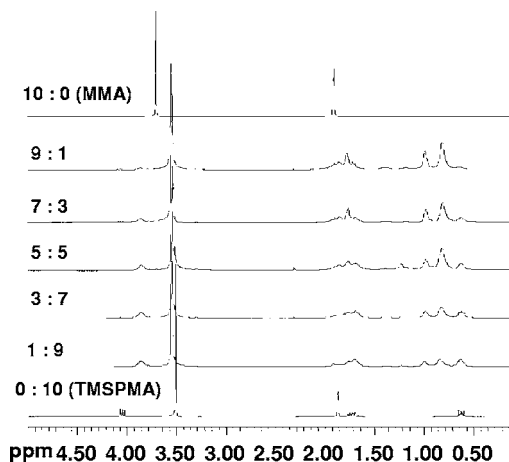


FIG. 3.  $^1\text{H}$ -NMR spectra of copolymers of MMA and TMSPMA with different  $x:y$  monomer proportions.

mer TMSPMA in the feed ( $f_{\text{TMSPMA}}$ ), and the molar fraction content of TMSPMA in the copolymers ( $F_{\text{TMSPMA}}$ ) are listed in Table I. Also included in this table are the molecular weights and polydispersion indices of the copolymers.

The monomer reactivity ratios (defined as the ratios of the rate constant for a given macroradical adding to its own monomer to that for its adding to the other monomer) for MMA/TMSPMA copolymerization in toluene solution were determined from both the monomer feed and the average composition of copolymers listed in the above table. Considering the Mayo-Lewis terminal model,<sup>25</sup> and using nonlinear least-squares analysis suggested by Tidwell and Mortimer,<sup>26</sup> the so obtained monomer reactivity ratio values were  $r_{\text{MMA}} = 0.66$  and  $r_{\text{TMSPMA}} = 0.50$ . The accuracy of the estimated data is represented in Fig. 4(a), where the 95% joint confidence interval is drawn (that is, the estimated error in the calculated reactivity relations). Figure 4(b) shows the experimental copolymer composition data and the curve calculated with the above obtained reactivity ratios. The diagonal line represents a copolymer with the same content of both monomers than the monomer mixture (monomer feed). It can be seen in Fig. 4(b) that the agreement between experimental data and calculated curve is quite satisfactory.

The close values of the reactivity ratios of both monomers and the diagram of the copolymer composition reflect that the random copolymers obtained show a certain tendency toward alternation and, therefore, a close composition

TABLE I. Molar fraction composition in the monomer feeds ( $f_{\text{TMSPMA}}$ ) and in the copolymer ( $F_{\text{TMSPMA}}$ ), conversion, number average ( $M_n$ ) and weight average ( $M_w$ ) molecular weights, and polydispersion index (PI) of copolymers.

$f_{\text{TMSPMA}}$	$F_{\text{TMSPMA}}$	Conversion (%)	$M_n$ (g/mol)	$M_w$ (g/mol)	PI
0.048	0.089	4.9	54 000	96 900	1.79
0.162	0.235	7.8	74 900	128 800	1.72
0.310	0.383	8.6	63 300	108 600	1.72
0.512	0.540	7.0	57 700	135 400	2.35
0.802	0.763	3.9	69 200	126 600	1.83
0.895	0.862	3.2	99 900	171 800	1.72

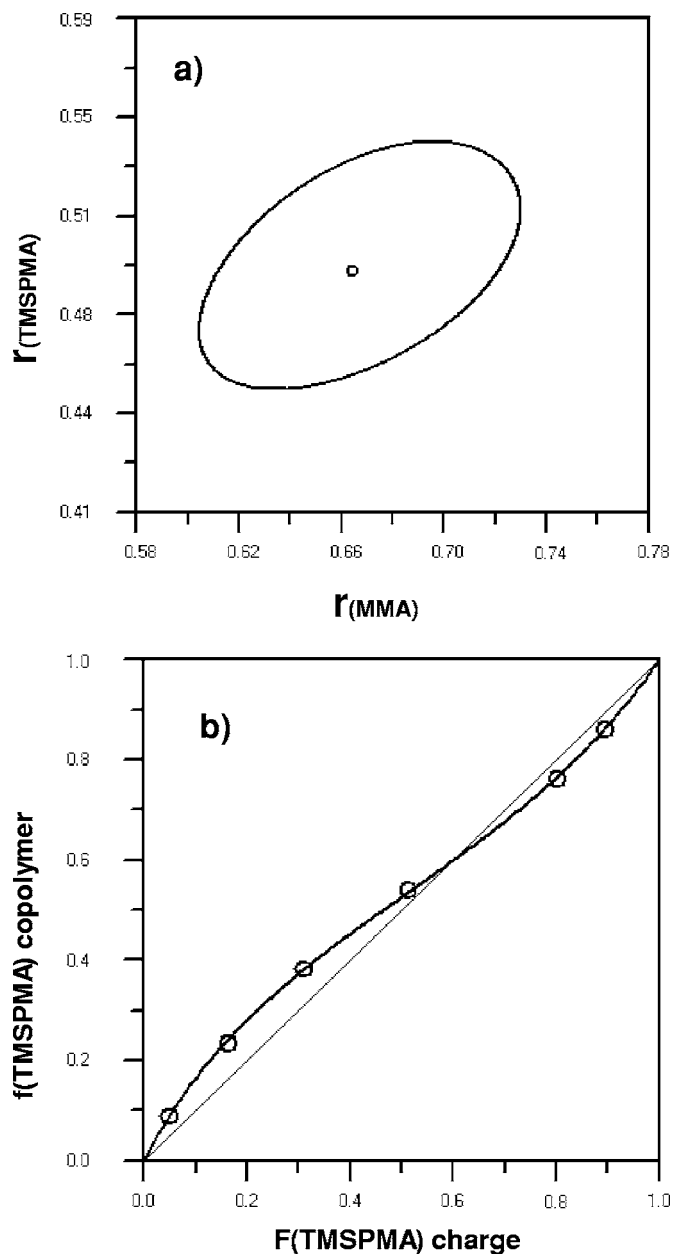


FIG. 4. (a) The 95% joint confidence interval (circle) of reactivity ratios ( $r_{\text{MMA}}$ ,  $r_{\text{TMSPMA}}$ ). (b) Experimental copolymer composition data as defined in Table I (open circles) and calculated curve (full line) obtained with the ( $r_{\text{MMA}}$ ,  $r_{\text{TMSPMA}}$ ) ratio showed in (a). The diagonal line represents a copolymer with the same content of both monomers than the monomer mixture (monomer feed).

and a monomer sequence distribution in the copolymers are obtained with all the monomer feed compositions employed.

The glass transition temperatures of the different materials, determined by DSC, are collected in Table II. As an example, in Fig. 5 are plotted the DSC thermograms for the COP(MMA-TMSPMA) compounds. Similar plots were obtained for the matrices based on HEMA and MMA-HEMA. The results presented in Table II and Fig. 5 indicate a decrease in  $T_g$  together with a lessening in the characteristic step in the heat capacity as the proportion of monomer TMSPMA in the matrix increases, which is an indication of the plasticizer effect of the alkoxide groups in TMSPMA.<sup>27</sup> In addition, this decrease of  $T_g$  with the increased content of

TABLE II. Glass transition temperatures ( $T_g$ ).

Matrix material	$T_g$ (°C)
PMMA	101
COP(MMA-TMSPMA 9:1)	93
COP(MMA-TMSPMA 8:2)	91
COP(MMA-TMSPMA 7:3)	84
COP(MMA-TMSPMA 5:5)	76
COP(MMA-TMSPMA 4:6)	55
COP(MMA-TMSPMA 3:7)	45
PHEMA	96
COP(HEMA-TMSPMA 9:1)	92
COP(HEMA-TMSPMA 8:2)	90
COP(HEMA-TMSPMA 7:3)	89
COP(HEMA-TMSPMA 5:5)	82
COP(HEMA-TMSPMA 4:6)	79
COP(MMA-HEMA)	90
TERP(MMA-HEMA-TMSPMA 7:3:10)	61
TERP(MMA-HEMA-TMSPMA 5:5:10)	63
TERP(MMA-HEMA-TMSPMA 3:7:10)	58

TMSPMA indicates that the degree of condensation between the alkoxide groups detected in the IR and NMR spectra of the prepared materials is quite low because a more significant formation of Si–O–Si bonds would result in an increase in the corresponding glass transition temperature. In the terpolymers TERP(MMA-HEMA-TMSPMA), where only the relative amounts of MMA and HEMA are varied and the amount of TMSPMA remains constant, the  $T_g$  also remains about constant, as to be expected from the constancy of the TMSPMA content. The existence of only one  $T_g$  in all cases indicates that the materials are structurally homogeneous.

The thermal stability of the silicon-modified organic materials was evaluated by TGA and derivative thermogravimetry (DTG) data. In Fig. 6 are represented the weight losses for the MMA-TMSPMA copolymers in nitrogen atmosphere as a function of temperature as well as the corresponding derivatives of the weight loss. Thermogram and its first derivative of the PMMA homopolymer are also included for comparison. It can be observed in Fig. 6 that all matrices incorporating the silicon-containing monomer TMSPMA begin to decompose at about 100 °C above the temperature at which the decomposition of the homopolymer PMMA be-

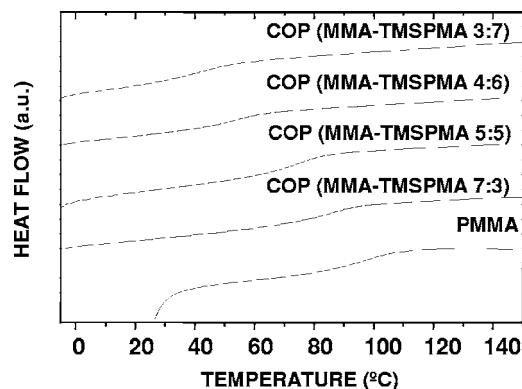


FIG. 5. DCS thermograms of COP(MMA-TMSPMA) matrices obtained at heating rate of 20 °C/min under nitrogen atmosphere. Thermogram of homopolymer PMMA is also included for comparison.

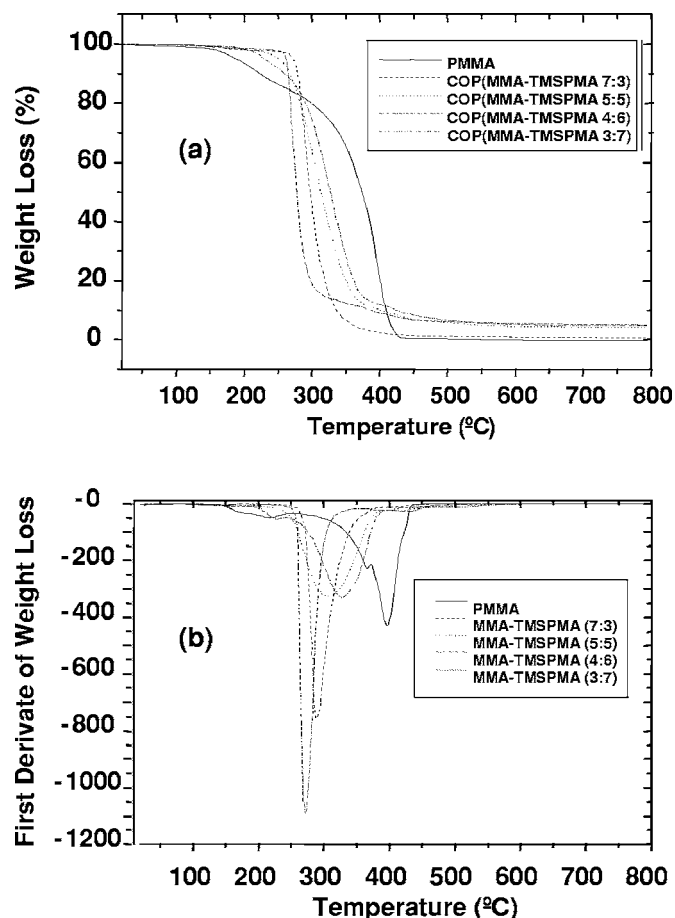


FIG. 6. TGA thermograms of COP(MMA-TMSPMA) matrices obtained at heating rate of 5 °C/min under nitrogen atmosphere (a) and corresponding first derivative curves (b). Thermogram and first derivative curve of homopolymer PMMA are also included for comparison.

gins. This is in agreement with previous reports which indicated an increase in the thermal stability of hybrid materials as a consequence of the increased cross-linking in the inorganic network and the interactions between organic and inorganic components.<sup>28</sup> Thus, the higher thermal stability of the silicon-modified materials would reflect the increase in the silicon content in these materials as well as a certain degree of condensation between the silanol groups in TMSPMA, enough to increase the thermal stability of the material but without increasing the glass transition temperature.

Once the MMA-TMSPMA copolymers begin to decompose, the rate of thermal degradation is higher than in the homopolymer. This could be an indication of a higher thermal conductivity in the copolymers than in the homopolymer PMMA. A more homogeneous distribution of the temperature in the silicon-modified materials would result in a homogeneous decomposition in these materials, whereas in PMMA the decomposition would begin in the outer layers of the sample, in direct contact with the oven environment.

Similar results were obtained with the HEMA-TMSPMA copolymers. In the terpolymers, the silicon-containing materials begin to decompose at about 50 °C above the temperature at which the organic copolymer begins to decompose, and then the rate of decomposition is

TABLE III. Refractive indices ( $n \pm 0.0005$ ) of the different dye-doped materials studied in this work, measured at the 589 nm Na line.

Matrix material	Dye	
	PM567 ( $1.5 \times 10^{-3} M$ )	PM597 ( $6 \times 10^{-4} M$ )
COP(MMA-TMSPMA 9:1)		1.4890
COP(MMA-TMSPMA 8:2)		1.4875
COP(MMA-TMSPMA 7:3)	1.4845	1.4842
COP(MMA-TMSPMA 5:5)	1.4822	1.4820
COP(MMA-TMSPMA 4:6)	1.4800	1.4800
COP(MMA-TMSPMA 3:7)	1.4760	1.4760
COP(HEMA-TMSPMA 9:1)	1.5087	1.5085
COP(HEMA-TMSPMA 8:2)	1.5050	1.5045
COP(HEMA-TMSPMA 7:3)	1.5025	1.5020
COP(HEMA-TMSPMA 5:5)	1.4995	1.5010
COP(HEMA-TMSPMA 4:6)	1.4910	1.4915
TERP(MMA-HEMA-TMSPMA 7:3:10)	1.4850	1.4850
TERP(MMA-HEMA-TMSPMA 5:5:10)	1.4890	1.4895
TERP(MMA-HEMA-TMSPMA 3:7:10)	1.4910	1.4910

slightly higher than that of the corresponding copolymer, with the behavior of the terpolymers being similar, reflecting that their silicon content is the same in all of them.

In Table III are collected the refractive indices ( $n$ ) of the different dye-doped compounds studied in this work. In Fig. 7, the values of the refractive index of the copolymers of MMA and TMSPMA doped with dye PM597 are plotted as a function of the silicon atom contents in the matrix. It is seen that  $n$  decreases linearly with the increasing content of silicon atoms, in agreement with previous reports.<sup>29</sup> The same behavior is observed in the copolymers of HEMA, and TMSPMA. In the terpolymers of MMA, HEMA, and TMSPMA, where the content of silicon atoms in the matrices remains constant, there is a small but systematic variation of the refractive index, which increases with the ratio HEMA/MMA, reflecting that poly(2-hydroxyethyl methacrylate) (PEHMA) is a material with higher refractive index than PMMA ( $n_{\text{PEHMA}} = 1.5119$ ;  $n_{\text{PMMA}} = 1.4900$ ). Thus, the refractive index of the silicon-modified organic matrices with a particular organic composition can be tuned by varying the

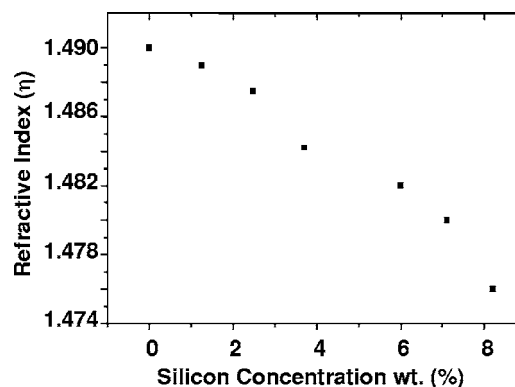


FIG. 7. Variation of the refractive index of MMA-TMSPMA copolymers doped with dye PM597 as a function of the content of silicon atoms in the matrix.

TABLE IV. Laser parameters [ $\lambda_{\max}$ : peak of the laser emission; Eff: energy conversion efficiency;  $I_{100\,000}(\%)$ : intensity of the dye laser output after 100 000 pump pulses in the same position of the sample, referred to initial intensity  $I_0$ .] for dyes PM567 and PM597 incorporated into different copolymers (COP) and terpolymers (TERP) with silicon atoms in their structure. Nd:YAG laser (second-harmonic) pump energy: 5.5 mJ/pulse.

Matrix material	PM567 ( $1.5 \times 10^{-3} M$ )				PM597 ( $6 \times 10^{-4} M$ )			
	$\lambda_{\max}$ (nm)	Eff (%)	$I_{100\,000}$ (%)		$\lambda_{\max}$ (nm)	Eff (%)	$I_{100\,000}$ (%)	
			10 Hz	30 Hz			10 Hz	30 Hz
COP(MMA-TMSPMA 9:1)					577	42	94	
COP(MMA-TMSPMA 8:2)					576	40	104	
COP(MMA-TMSPMA 7:3)	562	20	53		577	26	138	122
COP(MMA-TMSPMA 5:5) <sup>a</sup>	564	15	(70) <sup>b</sup>		578	20	120	117
COP(MMA-TMSPMA 4:6) <sup>a</sup>	560	21	112	50	575	22	100	
COP(MMA-TMSPMA 3:7)	562	14	120	8	575	12	76	
COP(HEMA-TMSPMA 9:1)	555	31	62		575	36	97	
COP(HEMA-TMSPMA 8:2)	562	34	77		578	32	100	
COP(HEMA-TMSPMA 7:3)	560	14	93		577	16	129	96
COP(HEMA-TMSPMA 5:5) <sup>a</sup>	559	14	(45) <sup>b</sup>		575	20	106	119
COP(HEMA-TMSPMA 4:6)	558	15	52		575	6	98	69
TERP(MMA-HEMA-TMSPMA 7:3:10)	562	16	98	74	577	15	108	116
TERP(MMA-HEMA-TMSPMA 5:5:10) <sup>a</sup>	560	10	(65) <sup>b</sup>		576	15	(110) <sup>b</sup>	106
TERP(MMA-HEMA-TMSPMA 3:7:10)	562	15	37		575	14	108	96

<sup>a</sup>These data were also presented in Ref. 19.

<sup>b</sup>Intensity of the laser output after 90 000 pump pulses in the same position of the sample, referred to initial intensity  $I_0$ .

silicon atom content, which could be of importance for potential applications of these materials in micro- and nanophotonic devices.

## B. Laser operation

Broadband laser emission, with beam divergences of the order of 5 mrad and pulse duration of about 5 ns (full width at half maximum) was obtained from all the materials under study. Oscillation bandwidths were of the order of 8 nm for PM567 (dye concentration of  $1.5 \times 10^{-3} M$ ) and 5 nm for PM597 (dye concentration of  $6 \times 10^{-4} M$ ).

Data for both pyrromethene dyes on lasing efficiency, peak of the laser emission, and intensity of the laser output (referred to initial intensity) after 100 000 pump pulses in the same position of the sample at 10 Hz repetition rate are collected in Table IV. To facilitate comparisons we have represented graphically in Figs. 8 and 9 some of the data for pyrromethene dyes.

### 1. Pyrromethene dyes

With pyrromethene dyes, for a given amount of TMSPMA in the matrix, the efficiencies were always higher in the copolymers with MMA (Table IV). The presence of HEMA in the matrix material resulted in a decrease in the lasing efficiency of both PM567 and PM597 dyes. This tendency had been previously observed when dye PM567 was incorporated into pure polymeric matrices of PMMA and PHEMA, where the lasing efficiencies were only 12% and 7%, respectively.<sup>20</sup>

Examination of Figs. 8 and 9 allows appreciating the general tendencies of the evolution of efficiency and photostability of the pyrromethene dyes as a function of the matrix

content of TMSPMA. With dye PM567 (Fig. 8), the lasing efficiency in the matrices containing TMSPMA was always higher than in the matrices based on both homopolymers PMMA and PHEMA. In the MMA-based copolymers, the photostability keeps on increasing with the content of TMSPMA, whereas the efficiency oscillates, with values around 18%, independently of the TMSPMA content. When the comonomer was HEMA, the photostability optimizes for

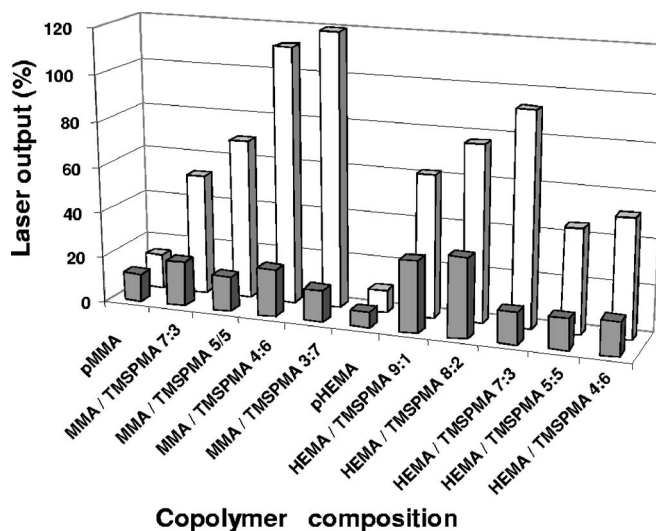


FIG. 8. Dependence on the content of TMSPMA in the COP(MMA-TMSPMA) matrices of the efficiency (dark columns) and stability (white columns) of the laser output of dye PM567. Stability measured as percent intensity, referred to initial intensity, of the laser output after 100 000 pump pulses in the same position of the sample. Results obtained in the homopolymers PMMA and PHEMA are also included for comparison. Dye concentration:  $1.5 \times 10^{-3} M$ . Pump energy and repetition rate: 5.5 mJ/pulse and 10 Hz, respectively.

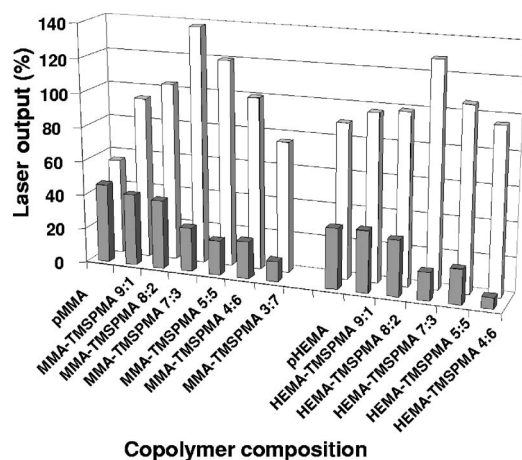


FIG. 9. Dependence on the content of TMSPMA in the COP(MMA-TMSPMA) matrices of the efficiency (dark columns) and stability (white columns) of the laser output of dye PM597. Stability measured as percent intensity, referred to initial intensity, of the laser output after 100 000 pump pulses in the same position of the sample. Results obtained in the homopolymers PMMA and PHEMA are also included for comparison. Dye concentration:  $1.5 \times 10^{-3} M$ . Pump energy and repetition rate: 5.5 mJ/pulse and 10 Hz, respectively.

the matrix composition HEMA-TMSPMA 7:3. Both higher and lower contents of TMSPMA result in noticeable decreases of stability. The lasing efficiency follows a similar pattern, although its peak value is obtained with a lower amount of silicon-containing monomer in the matrix.

From Fig. 8 and the more detailed data in Table IV, it can be concluded that the best overall laser performance of dye PM567 was obtained with the dye incorporated into material COP(MMA-TMSPMA 4:6), where the lasing efficiency was 21% and the laser emission was highly stable, with the intensity of the laser output remaining above the initial lasing intensity after 100 000 pump pulses in the same position of the sample. Although good stabilities were also obtained with other organically modified matrices (copolymers MMA-TMSPMA and HEMA-TMSPMA in *v/v* proportions of 3:7 and 7:3, respectively, or terpolymer of MMA, HEMA, and TMSPMA in proportions of 7:3:10), the lasing efficiencies in those matrices were lower. On the other hand, in those matrices with higher lasing efficiency (copolymers HEMA-TMSPMA in *v/v* proportions of 9:1 and 8:2), the photostability was clearly worst than in the COP(MMA-TMSPMA 4:6) material.

Finally, it can be appreciated in Table IV that in the terpolymers, where the proportion of TMSPMA is kept constant, the higher the content of HEMA is the lower the stability of the laser emission is, indicating once more that the presence of HEMA in the matrix worsens the lasing performance of the PM567 dye.<sup>30</sup>

The best results we had obtained in previous studies on dye PM567 incorporated into pure organic polymeric media were a lasing efficiency of 12% and a decrease of the laser output to 16% of the initial after just 30 000 pump pulses at 10 Hz repetition rate.<sup>31</sup> Comparison with the results in Table IV clearly shows the much improved laser performance obtained with the incorporation of silicon atoms in the matrix structure.

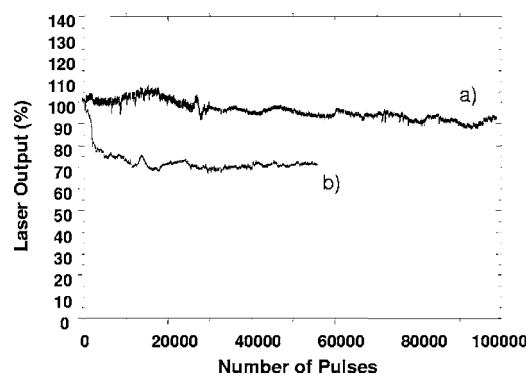


FIG. 10. Normalized laser output as a function of the number of pump pulses in the same position of the sample for dye PM567 incorporated into (a) COP(HEMA-TMSPMA 7:3) and (b) COP(HEMA-MMA 1:1) + 5 wt % of tetraethoxysilane. Dye concentration  $1.5 \times 10^{-3} M$ . Pump energy and repetition rate: 5.5 mJ/pulse and 10 Hz, respectively.

Some of the above results improve the already high photostability we had demonstrated for dye PM567 incorporated into organic-inorganic hybrid matrices while maintaining the lasing efficiency.<sup>11</sup> In Fig. 10 we compare the evolution of the laser output with the number of pump pulses for dye PM567 incorporated into one of the organically modified matrices studied in this paper with that of the same dye, under the same experimental conditions, in the best organic-inorganic hybrid combination previously studied.<sup>11</sup>

Recently, we developed hybrid materials for solid-state dye lasers based on highly porous silica aerogels.<sup>15</sup> In this approach, the open porous network of the aerogel was filled with adequate polymeric formulations incorporating the laser dye. Using dye PM567, we demonstrated highly stable laser operation (with the laser emission remaining at about 90% of its initial value after  $10^6$  pump pulses at 10 Hz repetition rate) but with low initial lasing efficiency (12%). Conditions were obtained where the lasing efficiency rose to 37%, but then the stabilities decreased to values similar to those obtained in this work. In all cases, the spatial quality of the laser emission from samples based on silica aerogels was clearly lower than that obtained with the here reported silicon-modified organic matrices, which exhibit a higher optical homogeneity than the hybrid ones. This, together with some other problems posed by hybrid materials related to the long periods of time required for the synthesis procedure (about two months as compared with the one to two weeks required for the preparation of the organic matrices), need for a careful control of the experimental conditions during the synthesis to avoid destruction of the dye molecules, and fragility of the final material, which makes it difficult and costly to obtain a proper finishing of the samples puts in a clear advantage the use of silicon-modified polymeric materials as matrices for lasing dyes under otherwise similar conditions of lasing performance.

For dye PM597 the lasing efficiencies varied from 6% to 42%, depending on the matrix composition, but in all cases the laser emission was remarkably stable, with no sign of degradation in the laser output in all but one of the materials tested after 100 000 pump pulses in the same position of the sample (Table IV). The behavior of dye PM597 in the ma-



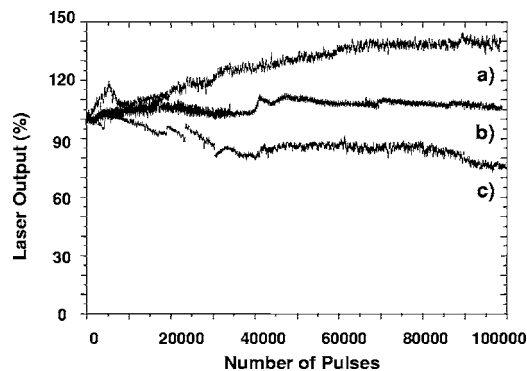


FIG. 11. Normalized laser output as a function of the number of pump pulses in the same position of the sample for dye PM597 incorporated into (a) COP(MMA-TMSPMA 7:3), (b) TERP(MMA-HEMA-TMSPMA 7:3:10), and (c) COP(MMA-TMSPMA 3:7). Dye concentration:  $6 \times 10^{-4}M$ . Pump energy and repetition rate: 5.5 mJ/pulse and 10 Hz, respectively.

trices with different proportions of TMSPMA can be more easily appreciated in Fig. 9, where the efficiencies and stabilities obtained with the dye incorporated into homopolymers PMMA and PHEMA are also included for comparison. It is seen that although the lasing efficiency steadily decreases with the content of the silicon-modified monomer in the matrix, the photostability follows a different pattern: it first increases and then decreases, with the highest photostability reached in both copolymers of MMA and HEMA with TMSPMA when the volume proportion of the silicon-modified monomer in the matrix is 30%. Thus, as in the case of PM567, the highest photostability is not reached in the material which optimizes the efficiency, and a compromise should be reached to combine high photostability with reasonable lasing efficiency.

In Fig. 11, examples are shown of the actual evolution of the laser output with the number of pump pulses for dye PM597 in three different matrices of those investigated in this work. In some of the materials tested, the laser emission exhibited a rather irregular behavior with some oscillations, first increasing and then decreasing until finally stabilizing with emission intensity above the initial intensity. This behavior could be related to the well-known fact that for each dye in a given medium there is an optimum concentration which results in the highest lasing efficiency.<sup>20</sup> Concentrations higher than the optimum cause a decrease in lasing efficiency. Because the degradation of dye molecules caused by repeated pumping in the same region of the sample produces a decrease in the effective dye concentration in that region, if the initial dye concentration were too high for the particular material used as host the result of the repeated pumping would be that the dye concentration would become nearer the optimum concentration, and thus the lasing efficiency would increase.

In previous studies we presented evidences showing that the accumulation of heat into the material in polymeric solid-state dye lasers increased significantly with the pump repetition rate, impairing lasing stability.<sup>32</sup> With dye PM567 incorporated into hybrid organic-inorganic materials, this effect showed a significant decrease in lasing photostability when the pump repetition rate increased from 5 to 10 Hz.<sup>11</sup> Thus,

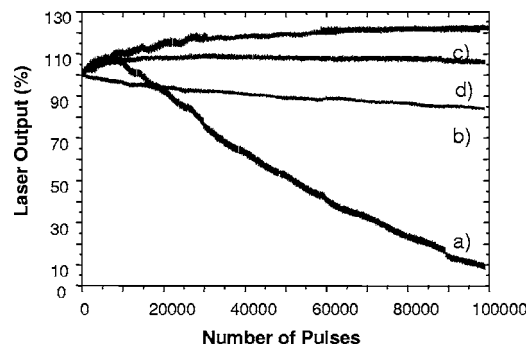


FIG. 12. Normalized laser output as a function of the number of pump pulses in the same position of the sample for dye PM567 incorporated into (a) COP/MMA-TMSPMA 3:7) and (b) COP(HEMA-TMSPMA 7:3) and for dye PM597 incorporated into (c) COP(MMA-TMSPMA 7:3) and (d) TERP(MMA-HEMA-TMSPMA 5:5:10). Dye concentration:  $1.5 \times 10^{-3}M$  (PM567) and  $6 \times 10^{-4}M$  (PM597). Pump energy and repetition rate: 3.5 mJ/pulse and 30 Hz, respectively.

to check the limits of photostability in the silicon-modified organic materials, we proceeded to pump at 30 Hz some of the materials which had shown good stability when pumped at 10 Hz. The results obtained are collected in Table IV. Figure 12 shows the actual evolution of the laser output at 30 Hz repetition rate of a representative selection of the materials in Table IV.

Under 30 Hz pumping the dye PM567 exhibits a steady decrease in the laser output with the number of pump pulses, which is rather drastic in the sample with the highest content of silicon [Figs. 12(a) and 12(b)]. Dye PM597 behaves much better, and stable laser output is obtained with all but one of the samples studied. The general tendencies are similar to those found under pumping at 10 Hz, and only in the copolymer of HEMA and TMSPMA with the highest content of silicon does the laser output decrease significantly with the number of pump pulses over the considered 100 000 pump pulses interval.

The above results confirm that dye PM597 clearly outperforms dye PM567 as laser dye in solid-state operation. Whereas both dyes exhibited close initial lasing efficiencies, dye PM597 was more stable under most circumstances (Figs. 8 and 9). Under the more demanding 30 Hz repetition rate, the higher thermal load produced by the increased repetition rate caused early degradation of dye PM567 but did not affect significantly the dye PM597 after 100 000 pump pulses in the same position of the sample.

The better laser performance of dye PM597 as compared with dye PM567 could be somewhat of a surprise, taking into account that the fluorescence quantum yield ( $\Phi$ ) of PM567 is much higher than that of PM597: in trifluoroethanol,  $\Phi$  (PM567)=0.97<sup>33</sup> whereas  $\Phi$  (PM597)=0.49.<sup>34</sup> A relevant difference between both dyes is that upon excitation the geometrical rearrangement of dye PM597 leads to a significant increase of the Stokes shift ( $\Delta\nu \approx 1250 \text{ cm}^{-1}$ ) with respect to that of PM567 ( $\Delta\nu \approx 500 \text{ cm}^{-1}$ ). This would reduce the losses in the resonator cavity by reabsorption/reemission effects, which are governed by the overlap between the absorption and the emission spectra and are of particular importance in the high optical density solid solutions here analyzed. Differences in thermal degradation and

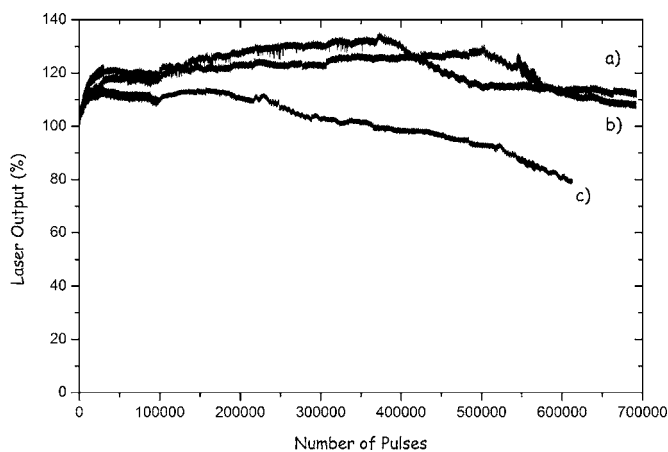


FIG. 13. Normalized laser output as a function of the number of pump pulses in the same position of the sample for dye PM597 incorporated into (a) COP/MMA-TMSPMA 5.5), (b) COP(HEMA-TMSPMA 5:5), and (c) TERP(MMA-HEMA-TMSPMA 5:5:10). Dye concentration:  $6 \times 10^{-4} M$ . Pump energy and repetition rate: 3.5 mJ/pulse and 30 Hz, respectively.

reactivity to singlet oxygen could also come into play.<sup>35,36</sup> To evaluate the role of these processes in the laser operation of the above pyromethene dyes, studies are in progress on their thermostability and photooxidation kinetics.

Trying to observe differences in the stability of the laser output in matrices incorporating dye PM597, we proceeded to pump three of the samples with the same content of silicon (50% proportion of TMSPMA) but differing in the organic part (which was either MMA, HEMA, or MMA-HEMA 5:5), at 30 Hz over a span of 700 000 pump pulses in the same position of the sample (Fig. 13). It can be seen that only in the terpolymer is there a significant decrease in the laser output, and even then the laser emission remains at 76% of the initial value after 700 000 pump pulses in the same position of the sample. In both MMA-TMSPMA and HEMA-TMSPMA copolymers, the laser output first increases slowly and steadily over the first 400 000–500 000 pump pulses to decay somewhat later on, but still remains at about or over the initial level after 700 000 pump pulses in the same position of the sample, exhibiting a most remarkable stability.

Our best previous results obtained with dye PM597 incorporated into hybrid matrices consisting of copolymers of MMA and HEMA 1:1 with up to 15 wt % of methyltriethoxysilane (TRIEOS) were lasing efficiencies of up to 23% and stabilities under 10 Hz pump repetition rates similar to those obtained in the present work.<sup>16</sup> However, when those matrices were pumped at 30 Hz repetition rate, the laser output in the matrix with better performance dropped to 33% of the initial emission after only 60 000 pump pulses.

When comparing our results with the efficiency results obtained by other authors, some care should be taken because our studies have been performed under transversal pumping and with the oscillator cavity not optimized. Thus, although lasing efficiencies as high as 79% and 60% have been reported for dyes PM567 and PM597, respectively, incorporated via the sol-gel technique into organically modified silicate (ORMOSIL) host matrices (PM567) (Ref. 12) and hybrid xerogel matrices (PM597),<sup>10</sup> those efficiencies were obtained under longitudinal pumping in optimized laser

cavities. Under transversal pumping, slope efficiencies of 32% (Ref. 8) and 43% (Ref. 14) have been obtained for dyes PM567 and PM597, respectively, incorporated into ORMOSIL glass samples and placed in an optimized laser cavity consisting of a full reflector and a 50% broadband reflector as output coupler.

Likewise, proper comparison of stability results obtained by different authors is a difficult task because of the substantial differences in experimental conditions, such as repetition rate or pumping configuration, which can strongly affect the longevity of the solid samples. In order to facilitate comparisons independent of the experimental setup, Rahn and King<sup>37</sup> introduced a normalized photostability defined as the accumulated pump energy absorbed by the system per mole of dye molecules before the output energy falls to one-half its initial value. Its units are GJ/mol. In these units, the best previous results for PM567 photostability in solid matrix have been reported by Ahmad *et al.*,<sup>38</sup> who obtained a normalized photostability of 350 GJ/mol for a mixture of PM567 and Coumarin 540 in polymer samples longitudinally pumped at 532 nm with pulses at a fluence of 1 J/cm<sup>2</sup> and 10 Hz repetition rate. In our case, we estimate that the accumulated pump energy absorbed per mole of dye PM567 after the 100 000 pump pulses was 518 GJ/mol, with the laser output energy remaining at the initial level when the matrix was COP(MMA-TMSPMA 4:6). When the same matrix was pumped at 30 Hz, we obtained a normalized photostability of 989 GJ/mol.

With dye PM597 incorporated into hybrid xerogel matrices and pumped longitudinally at 532 nm with 1.8 mJ/pulse at 10 Hz repetition rate, Nung *et al.*<sup>10</sup> reported a drop in the laser emission to 75% of its initial value after 100 000 pump pulses. As reported above, we obtained the same dye laser emission with no sign of degradation in the laser output in all but one of the materials tested after 100 000 pump pulses, corresponding to an absorbed pump energy of 1295 GJ/mol. In measurements at 30 Hz repetition rate, the laser emission from dye PM597 in matrices based on copolymers of MMA and HEMA with TMSPMA in proportion of 5:5 remained at the initial level when the absorbed pump energy was 17 300 GJ/mol.

To assess the tuning capabilities of the developed materials, dyes PM567 and PM597 incorporated into COP(MMA-TMSPMA 4:6) matrices were placed in a grazing-incidence grating cavity in Shoshan configuration. Under these conditions, tunable laser emission with line-width of the order of 0.15 cm<sup>-1</sup> was obtained. Tuning ranges of 31 nm were observed with both dyes: from 553 to 584 nm with PM567 and from 567 to 598 nm with PM597.

#### IV. CONCLUSIONS

The silicon-modified organic matrices studied in this work have been characterized by using a number of optical microscopy and thermal and resonance techniques. The silicon content, thermal behavior, structure, and composition of the different materials have been evaluated. Densities varied between 1.17 and 1.20 g/cm<sup>3</sup>, depending on the particular matrix composition. Refractive indices were found to de-

crease linearly with the increasing content of silicon atoms. Thus, the refractive index of the silicon-modified organic matrices with a particular organic composition can be tuned by varying the content of silicon atoms, which could be of importance for potential applications of these materials in micro- and nanophotonic devices.

The results presented in this work indicate that the photostability of the laser operation of organic dyes incorporated into polymeric matrices is greatly enhanced by properly incorporating silicon atoms into the structure of the organic monomers. The matrix would remain organic, which means plasticity and easy synthesis, but with improved thermal properties due to the presence of the silicon atoms. Reasonable lasing efficiencies for laser operation under transversal pumping in no optimized laser cavities were obtained for pyrromethene dyes, and highly stable laser operation with no sign of degradation in the laser output after 100 000 pump pulses in the same position of the samples at 10 Hz repetition rate was demonstrated for both PM567 and PM597 laser dyes. This corresponds to an accumulated pump energy absorbed by the system per mole of dye molecules of 518 and 1295 GJ/mol for PM567 and PM597, respectively.

When the pump repetition rate was increased to 30 Hz, the dye PM567 exhibited a steady decrease in the laser output and it exhibited a normalized photostability (corresponding to a decrease of the laser output by 50%) of 989 GJ/mol. Dye PM597 was demonstrated to be much more stable than dye PM567, and in all but one of the matrices studied in this work its laser output remained stable after 100 000 pump pulses in the same position of the sample under pumping at 30 Hz (corresponding to an accumulated pump energy of 2472 GJ/mol). In two selected matrices, the laser emission of the dye PM597 remained stable after 700 000 pump pulses in the same position of the sample at 30 Hz repetition rate, corresponding to an accumulated pump energy absorbed by the system per mole of dye molecules of 17 300 GJ/mol.

When selected samples incorporating PM567 and PM597 dyes were placed in a wavelength-selective resonator, a narrow-linewidth operation with tuning ranges of up to 31 nm was obtained.

The remarkable improvement in photostability exhibited by the silicon-modified organic matrices under the demanding conditions of tightly focused transversal pumping makes the approach used in this work very promising in stabilizing the laser emission of dyes incorporated into solid matrices. The materials investigated in this work avoid some of the shortcomings of the organic hosts for solid-state dye lasers and, thus, could be excellent candidates for the implementation of solid matrices competitive with their liquid counterparts.

## ACKNOWLEDGMENTS

This work was supported by Project Nos. 7N/0100/02 of the Comunidad Autónoma de Madrid (CAM) and MAT2004-04643-C03-01 of the Spanish CICYT. One of the authors (O.G.) thanks the MEC for awarding her a Ramón y Cajal scientific contract. Another author (D.A.) thanks CAM for

a predoctoral scholarship. The authors also acknowledge Leoncio Garrido for expert help in the NMR measurements.

- <sup>1</sup>A. Costela, I. García-Moreno, and R. Sastre, in *Handbook of Advanced Electronic and Photonic Materials and Devices*, edited by H. S. Nalwa (Academic, San Diego, 2001), Vol. 7, pp. 161–208.
- <sup>2</sup>F. J. Duarte, *Appl. Opt.* **33**, 3857 (1994).
- <sup>3</sup>M. D. Rahn and T. A. King, *J. Mod. Opt.* **45**, 1259 (1998).
- <sup>4</sup>R. Sastre and A. Costela, *Adv. Mater.* (Weinheim, Ger.) **7**, 198 (1995).
- <sup>5</sup>W. Wunderlich, in *Polymer Handbook* (Wiley, New York, 1989), p. 77.
- <sup>6</sup>F. J. Duarte, A. Costela, I. García-Moreno, and R. Sastre, *Appl. Opt.* **39**, 6522 (2000).
- <sup>7</sup>F. J. Duarte, A. Costela, I. García-Moreno, R. Sastre, J. J. Ehrlich, and T. S. Taylor, *Opt. Quantum Electron.* **19**, 461 (1997).
- <sup>8</sup>E. Yariv and R. Reisfeld, *Opt. Mater.* (Amsterdam, Neth.) **13**, 49 (1999).
- <sup>9</sup>A. Costela, I. García-Moreno, C. Gómez, O. García, and R. Sastre, *Appl. Phys. B: Lasers Opt.* **75**, 827 (2002).
- <sup>10</sup>T. H. Nung, M. Canva, T. T. A. Dao, F. Chaput, A. Brun, N. D. Hung, and J. P. Boilot, *Appl. Opt.* **42**, 2213 (2003).
- <sup>11</sup>A. Costela, I. García-Moreno, C. Gómez, O. García, and R. Sastre, *Chem. Phys. Lett.* **369**, 656 (2003).
- <sup>12</sup>Y. Yang, M. Wang, G. Qian, Z. Wang, and X. Fan, *Opt. Mater.* (Amsterdam, Neth.) **24**, 621 (2004).
- <sup>13</sup>A. Costela, I. García-Moreno, C. Gómez, O. García, L. Garrido, and R. Sastre, *Chem. Phys. Lett.* **387**, 496 (2004).
- <sup>14</sup>R. Reisfeld, A. Weiss, T. Saraidarov, E. Yariv, and A. A. Ishchenko, *Polym. Adv. Technol.* **15**, 291 (2004).
- <sup>15</sup>A. Costela, I. García-Moreno, C. Gómez, O. García, R. Sastre, A. Roig, and E. Molins, *J. Phys. Chem. B* **109**, 4475 (2005).
- <sup>16</sup>I. García-Moreno, A. Costela, A. Cuesta, O. García, D. del Agua, and R. Sastre, *J. Phys. Chem. B* **109**, 21618 (2005).
- <sup>17</sup>F. J. Duarte and R. O. James, *Opt. Lett.* **28**, 2088 (2003).
- <sup>18</sup>F. J. Duarte and R. O. James, *Appl. Opt.* **43**, 4088 (2004).
- <sup>19</sup>A. Costela, I. García-Moreno, D. del Agua, O. García, and R. Sastre, *Appl. Phys. Lett.* **85**, 2160 (2004).
- <sup>20</sup>A. Costela, I. García-Moreno, and R. Sastre, *Phys. Chem. Chem. Phys.* **5**, 4745 (2003).
- <sup>21</sup>I. Soshan, N. N. Danon, and U. Oppenheim, *J. Appl. Phys.* **48**, 4495 (1977).
- <sup>22</sup>M. Rodríguez, A. Costela, I. García-Moreno, F. Florido, J. M. Figuera, and R. Sastre, *Meas. Sci. Technol.* **6**, 971 (1995).
- <sup>23</sup>P. Hajji, L. David, J. F. Gerard, J. P. Pascault, and G. Vigier, *J. Polym. Sci., Part B: Polym. Phys.* **37**, 3172 (1999).
- <sup>24</sup>M. Oubaha, M. Smaïhi, P. Etienne, and P. Y. Moreau, *J. Non-Cryst. Solids* **318**, 305 (2003).
- <sup>25</sup>F. R. Mayo and F. M. Lewis, *J. Am. Chem. Soc.* **66**, 1594 (1944).
- <sup>26</sup>P. W. Tidwell and G. A. Mortimer, *J. Macromol. Sci. Rev. Macromol. Chem.* **C4**, 281 (1970).
- <sup>27</sup>G.-H. Hsiue, W.-J. Kuo, Y.-P. Huang, and R.-J. Jeng, *Polymer* **41**, 2813 (2000).
- <sup>28</sup>C. K. Chang, I. M. Chu, W. Lee, and W. K. Chin, *Macromol. Chem. Phys.* **202**, 911 (2001).
- <sup>29</sup>Y.-Y. Yu and W.-Ch. Chen, *Mater. Chem. Phys.* **82**, 388 (2003).
- <sup>30</sup>A. Costela, I. García-Moreno, J. Barroso, and R. Sastre, *Appl. Phys. B: Lasers Opt.* **70**, 367 (2000).
- <sup>31</sup>A. Costela, I. García-Moreno, C. Gómez, F. Amat-Guerri, M. Liras, and R. Sastre, *Appl. Phys. B: Lasers Opt.* **76**, 365 (2003).
- <sup>32</sup>R. Duchowicz, L. B. Scaffardi, A. Costela, I. García-Moreno, R. Sastre, and A. U. Acuña, *Appl. Opt.* **42**, 1029 (2003).
- <sup>33</sup>A. Costela *et al.*, *J. Phys. Chem. A* **106**, 7736 (2002).
- <sup>34</sup>J. Bañuelos Prieto, F. López Arbeloa, V. Martínez Martínez, T. Arbeloa López, and I. López Arbeloa, *J. Phys. Chem. A* **108**, 5503 (2004).
- <sup>35</sup>M. D. Rahn, T. A. King, A. A. Gorman, and I. Hamblett, *Appl. Opt.* **36**, 5862 (1997).
- <sup>36</sup>M. Ahmad, M. D. Rahn, and T. A. King, *Appl. Opt.* **38**, 6337 (1999).
- <sup>37</sup>M. D. Rahn and T. A. King, *Appl. Opt.* **34**, 8260 (1995).
- <sup>38</sup>M. Ahmad, T. A. King, D. Ko, B. H. Cha, and J. Lee, *Opt. Laser Technol.* **34**, 445 (2002).